Biophysical Chemistry 187–188 (2014) 33–42

Contents lists available at ScienceDirect

Biophysical Chemistry

journal homepage: http://www.elsevier.com/locate/biophyschem

Exploring binding properties of naringenin with bovine β-lactoglobulin: A fluorescence, molecular docking and molecular dynamics simulation study

Samira Gholami, Abdol-Khalegh Bordbar *

Department of Chemistry, University of Isfahan, Isfahan 81746-73441, Iran

HIGHLIGHTS

- Naringenin quenches the fluorescence of BLG via static mechanism.
- The formation of 1:1 complex and high binding affinity of NG to BLG was assigned.
- The binding proceeded via hydrogen bonding and van der Waals interactions.
- The binding has insignificant changes in the secondary structure of protein.
- Both the correlated and anticorrelated motions increased during the binding process.

GRAPHICAL ABSTRACT

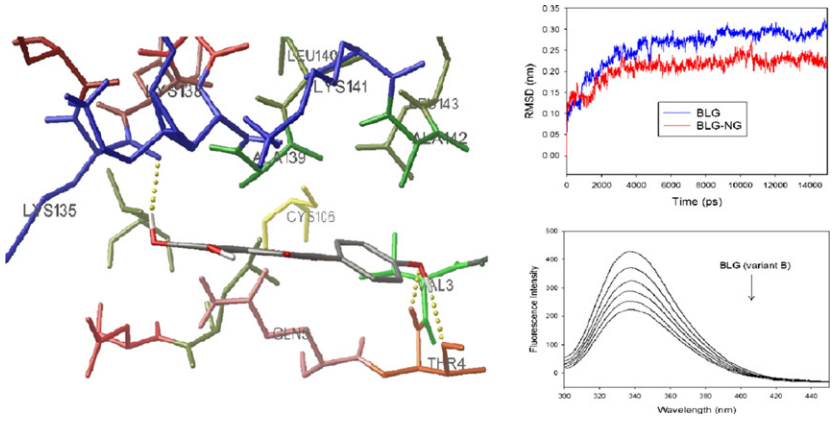

ARTICLE INFO

Article history:
Received 1 December 2013
Received in revised form 16 January 2014
Accepted 16 January 2014
Available online 28 January 2014

Keywords:
β-Lactoglobulin
Naringenin
Fluorescence quenching
Binding parameter
Molecular modeling

ABSTRACT

In the present study, the binding properties of naringenin (NG) to β-lactoglobulin (BLG) were explored using spectrofluorimetric and molecular modeling techniques. Analysis of spectrofluorimetric titration data represented the formation of 1:1 complex, significant binding affinity, negative values of entropy and enthalpy changes and the essential role of hydrogen bonding and van der Waals interactions in binding of NG to BLG. The value of determined Förster's distance represents the static mechanism for quenching of BLG by NG. The results of fluorescence competitive binding experiments characterize the location of NG binding site in the outer surface of BLG. Molecular docking study showed that NG binds in the outer surface site of BLG which is accompanied with three hydrogen bonds. The support of molecular docking results by biochemical fluorescence experiments confirms the validity of docking calculation. Analysis of molecular dynamics results indicated that NG can interact with BLG without affecting the secondary structure of protein.

1. Introduction

Flavonoids are a group of polyphenolic compounds (2-phenyl benzopyran skeleton) that are one of the common components in the human diet. They occur in fruit, vegetables, nuts, seeds, flowers, and bark. Flavonoids exhibit a wide range of biological effects including antioxidant, antibacterial, antiviral, antiinflammatory, antiallergic,

* Corresponding author. Tel.: +98 311 7932710, +98 9131677331; fax: +98 311 6689732.
E-mail addresses: bordbar@chem.ui.ac.ir, akbordbar@gmail.com (A.-K. Bordbar).

0301-4622/$ – see front matter © 2014 Elsevier B.V. All rights reserved.
http://dx.doi.org/10.1016/j.bpc.2014.01.003

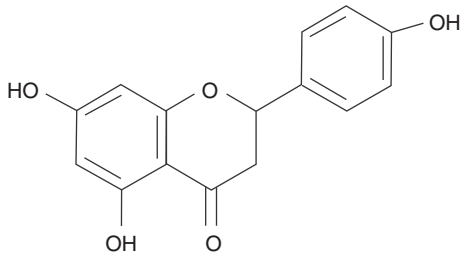

Scheme 1. Structure of naringenin (NG).

antistrogenic, anticarcinogenic activities [1–4]. Naringenin (NG; 4′,5,7-trihydroxyflavonone; Scheme 1), which belongs to flavonones, is one of the predominant bioflavonoids, which naturally occurs in citrus fruits, such as lemons, oranges and grapefruit [5]. NG is an excellent metal chelator and its complex with rare earth metals is reported to bind with the DNA, thus it can be considered as an antitumor drug via the inhibition of DNA activities [6]. The main challenge in the study and application of NG is its low bioavailability due to its poor water solubility [7]. Bioavailability of flavonoids can be increased via the use of proteins able to complex flavonoids.

Bovine β-lactoglobulin (BLG), a major whey protein in milk, belongs to the family of lipocalin proteins. It can bind with many hydrophobic nutrients and drugs such as fatty acids, lipids, aromatic compounds, vitamins and polyamines [8–10]. For oral delivery applications, because of good biocompatibility and biodegradability of milk proteins, BLG could be considered as a natural carrier for lipid-soluble drugs. Hence, BLG would be a suitable carrier for NG and related flavonoids and should improve the solubility and bioavailability of these drugs.

Fluorescence spectroscopy is a useful method to study the protein–drug interactions. It makes the determination of binding parameters and mechanism possible. In previous studies, interactions of NG and other flavonoids with the human (HSA) and bovine (BSA) serum albumin proteins have been investigated using spectroscopic techniques. For instance, it has been shown that the binding of diosmetin to HSA was driven mainly by hydrophobic interactions and hydrogen bonds and HSA conformation was slightly altered in the presence of diosmetin [11]. The results obtained from the binding studies of three flavonoids including naringenin, hesperetin and apigenin to BSA revealed that one flavonoid had an obvious effect on the binding of another flavonoid to protein when they coexisted in the BSA solution [12] and site marker competitive displacement experiments demonstrate that naringenin binds with high affinity to site I of BSA [13]. Furthermore, a computational study on the interaction of naringin palmitate with HSA [14], quercetin with β-casein micelles [15], and resveratrol, genistein, and curcumin with milk α- and β-caseins [16] has made it feasible to provide more information about the binding process at molecular level. Despite these relatively comprehensive studies on the complex formation of flavonoids and serum albumin proteins, there are a few reports on interaction of flavonoids with BLG. In this regard, the interaction of some flavonoids with bovine and reindeer BLG was studied using spectroscopic techniques [17]. The results showed that flavonols and flavanones bound to BLG with higher affinity than flavones and isoflavonols. Also, the relationship between the structural properties of some flavonoids and their affinities for milk proteins (MP) was investigated using spectrofluorimetric methods [18]. The results verified that the binding affinities to MP were strongly influenced by the structural changes of flavonoids, so that the methylation and methoxylation of flavonoids decreased affinities; the hydroxylation on the rings A and B of flavones and flavonols slightly enhanced the interaction; and the hydroxylation on the ring A of flavanones significantly improved the affinities. However, there is not any comprehensive experimental and computational study on complexation of BLG with NG in the literature.

In the present study, the interaction of NG with BLG was investigated in order to obtain an in-depth molecular understanding of binding mechanism by using spectrofluorimetric, molecular docking and molecular dynamics simulation methods. The number of binding sites, binding affinity, and thermodynamics parameters for BLG–NG complexation process were obtained from the analysis of spectrofluorimetric titration data. The binding site on BLG and the effect of complexation on the conformational stability and the secondary structure of BLG are reported here using the analysis of molecular docking and molecular dynamics simulation results.

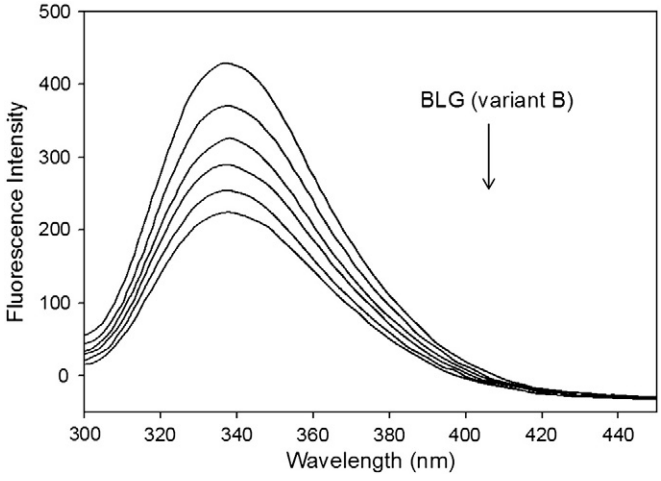

Fig. 1. Emission spectra of BLG in the presence of various concentrations of NG, c (BLG) = 10 μ M; c (NG), from 0 to 6 μM (T = 298 K, λ_{ex} = 280 nm). The arrow shows the increase of NG concentration.

2. Materials and methods

2.1. Materials

BLG (variant B > 99% purity) was purchased from Sigma Chemical Company and used without further purification. Retinol *all-trans* (R7632) and NG in analytical grade were purchased from Sigma. Phosphate buffers (PBS, 10 mM, pH 7.4 and pH 2.0) containing 0.075 M NaCl were used to keep constant pH value and the ionic strength. All used salts for buffer preparation were of analytical grade and were dissolved in deionized water. Ethanol was obtained from Merck Company.

2.2. Preparation of stock solutions

Protein stock solution (5 mg/mL) was prepared by dissolving BLG in 10 mM PBS. It was diluted to 0.2 mg/mL for fluorescence studies before being used. The protein concentration was determined spectrophotometrically using the extinction coefficient of 17,600 M^{-1} cm^{-1} at 280 nm [19]. NG stock solution (0.05 mg/mL) and retinol (RE) stock solution (0.01 mg/mL) were made in 10 mM PBS.

2.3. Fluorescence spectroscopy

All fluorescence spectra were obtained from a Shimadzu RF-5000 (Kyoto, Japan) Spectrofluorimeter equipped with a Xenon lamp source, 1.0 cm quartz cell and a thermostat bath that keep temperature constant within ±0.1 °C. The width of slit for both the excitation and emission was set at 5.0 nm. The emission spectra were recorded at λ_{ex} = 280 nm and λ_{em} from 300 to 450 nm and the intensity at 337.6 nm (maximum emission wavelength) was used to calculate the binding constants. In typical experiment, 1.5 mL of 0.2 mg/mL (10 μM) of protein solution was placed into the cuvette and was titrated manually by

successive additions of 0.05 mg/mL of NG stock solution. The fluorescence intensities were corrected for dilution effects, before they are considered for data analysis. In order to identify the location of the NG binding site, the same conditions and concentrations were used to design the ligand binding competition experiment. The competition for BLG binding site was studied by adding RE stock solution to BLG saturated before with NG.

The fluorescence quenching that may be occurred via static or dynamic mechanism is described by the Stern–Volmer equation [20]:

$$F_0/F = 1 + k_Q\tau_0[Q] = 1 + K_{sv}[Q]. \quad (1)$$

In this equation, F_0 and F are the fluorescence intensities in the absence and presence of quencher, respectively, K_{sv} is the Stern–Volmer quenching constant which can be written as $K_{sv} = k_Q\tau_0$ where k_Q is the biomolecular quenching rate constant and τ_0 is the average lifetime of the biomolecule without quencher ($\tau_0 = 10^{-8}$ s [21]) and [Q] is the concentration of the quencher.

In the case of static quenching, the number of substantive binding sites, n, and apparent binding constant of protein–ligand complex, K_a, can be determined by the following equation [22]:

$$\ln(F_0 - F)/F = \ln K_a + n \ln[Q]. \quad (2)$$

The most common application of fluorescence resonance energy transfer (FRET) is to measure the distance between two sites on a macromolecule. According to the Förster's theory the efficiency of energy transfer, E, is described by the following equation [20]:

$$E = 1 - (F/F_0) = R_0^6/\left(R_0^6 + r^6\right). \quad (3)$$

F_0 and F are the fluorescence intensity of protein in the absence and presence of equimolar concentration of acceptor (ligand), r is the distance from the bound ligand on protein to the tryptophan residue, and R_0 is the Förster critical distance at which 50% of the excitation energy is transferred to the acceptor and can be calculated by the following equation [20]:

$$R_0^6 = 8.79 \times 10^{-5}\kappa^2 N^{-4} Q_D J(\lambda) \quad \left(\text{in } Å^6\right) \quad (4)$$

where κ^2 is a factor describing the relative orientation of the transition dipoles of the donor and acceptor, N is the refractive index of medium, Q_D is the quantum yield of donor in the absence of acceptor and overlap integral J expresses the extent of overlap between the normalized fluorescence emission spectrum of the donor and the acceptor absorption spectrum. J is given by the following equation:

$$J = \sum F_D(\lambda)\varepsilon_A(\lambda)\lambda^4\Delta\lambda / \sum F_D(\lambda)\Delta\lambda. \quad (5)$$

$F_D(\lambda)$ is the fluorescence intensity of the fluorescent donor at wavelength λ and is dimensionless; $\varepsilon_A(\lambda)$ is the molar absorption coefficient of the acceptor at wavelength λ.

Table 1
Stern–Volmer constant, K_{SV} and biomolecular quenching rate constant, k_Q for NG with BLG.

Temperature (K)	K_{sv} (10^6 M^{-1})	k_Q (10^{14} M^{-1} S^{-1})	R^2
288	0.1455	0.1455	0.9857
293	0.1400	0.1400	0.9883
298	0.1370	0.1370	0.9976
303	0.1355	0.1355	0.9988

R^2 is regression coefficient.

2.4. Molecular docking

The structure of BLG was taken from Brookhaven Protein Data Bank (http://www.rcsb.org/pdb). Unliganded form of BLG (variant B), 3NPO, was chosen because it has no missing atom, no crystallized ligand and has a reasonable resolution. In order to get the optimized and stable geometry of ligand, the structure of NG was optimized by the quantum chemistry software Gaussian 03 using the Hartree–Fock method and 6-31G** basis set [23] and the structure with the lowest energy was chosen c for docking study. Docking calculations were done using AutoDock 4.2 program package. Firstly, *AutoDockTools* was used for the preparation of coordinate files of ligand and protein (PDBQT). Water molecules were removed from the structure of protein and Gastieger charges and missing hydrogen atoms were added to the BLG in AutoDockTools environment. Then, using *AutoGrid*, pre-calculation of grid maps of interaction energies for various ligand's atom types, such as aliphatic carbons, aromatic carbons, hydrogen bonding oxygens, and so on, so called 'probe', with protein has been done in order to save a lot of time during the docking. Each point within the grid map stores the potential energy experienced by 'probe' due to all the atoms in the protein. Finally, docking of NG to the BLG has been done using *AutoDock*. In this study docking experiments were performed using the AutoDock empirical free energy scoring function and the Lamarckian genetic algorithm with local search [24]. The amount of independent docking runs

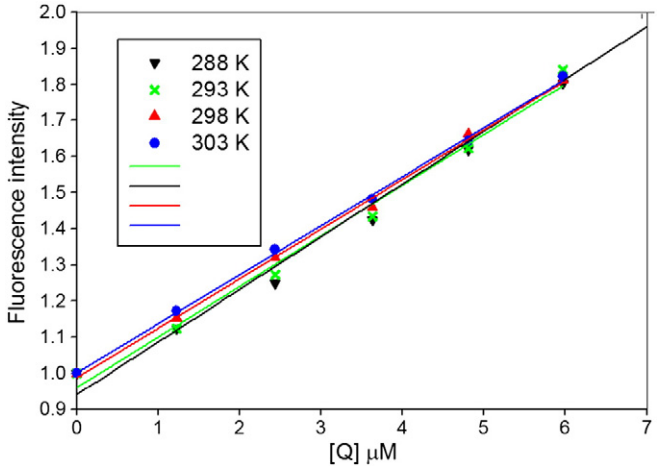

Fig. 2. Stern–Volmer curves for quenching of BLG by NG at different temperatures.

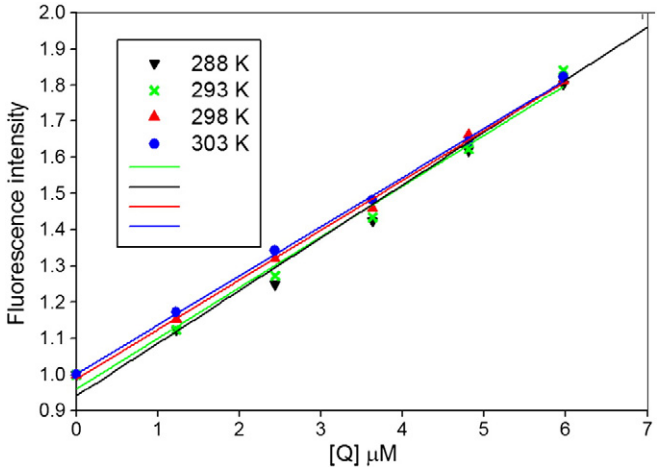

Fig. 3. Variation of $\ln((F_0 - F)/F)$ vs. $\ln[Q]$ for binding of NG to BLG at various temperatures.

Table 2
The apparent binding constants, K_a, number of binding sites, n, and thermodynamic parameters of binding for interaction of NG with BLG at different temperatures.

Temperature (K)	K_a (10^6 M^{-1})	n	R^2	$\Delta G°$ (kJ/mol)	$\Delta H°$ (kJ/mol)	$\Delta S°$ (J/mol · K)
288	2.5602	1.2432	0.9956	−35.3179	−110.3287	−260.454
293	1.4734	1.1980	0.9981	−34.5912		−258.490
298	0.5685	1.1144	0.9956	−32.8278		−260.070
303	0.2782	1.0536	0.9871	−31.5648		−259.947

performed for each docking simulation was set to 200 with 25,000,000 energy evaluations for each run and other docking parameters were set to the default. A blind docking with 126 point lattice along *X*, *Y*, and *Z* axes was performed to find the active site of NG to the BLG. After determination of the active site, the center of the grid set at the Cα atom of Leu(140) residue and the dimensions of the grid map were selected 60 points with a grid point spacing of 0.375 Å, to allow the ligand to rotate freely.

2.5. Molecular dynamics simulation

The binding modes of ligand to the protein, the binding energy and the residues of protein involved in the interaction with the ligand can be obtained from the docking method but, as in the docking studies, flexibility of the protein is not taken into consideration, it cannot give insight into the dynamics of binding process. In order to confirm the main binding mode of ligand and to give the whole impression of NG to the BLG, we performed MD simulations. Molecular dynamics simulation can account for further study of binding modes of ligand such as investigating and explaining the conformational changes of protein and the stability of complex during the binding. Hence, the geometry obtained from docking was used as starting conformation for molecular dynamics study.

A 15 ns MD simulation of the complex BLG–NG was carried out with the GROMACS4.5.4 package with the GROMOS96 43a1 force field [25]. The topology parameters of protein were created by using the Gromacs program. Single point charge (SPC) model was selected for water molecules [26]. The system was neutralized by adding the appropriate number of Na^+ counter-ions instead of solvent molecules. Finally, protein–ligand system was immersed in a cubic box (6.65049 × 6.65049 × 4.70261 nm^3) and the entire system was composed of 1594 atoms of BLG, one molecule of NG, 8 Na^+ counter-ions and 18,030 solvent atoms. 3D periodic boundary conditions were applied. The force field parameters for ligand were obtained from PRODRG web server [27].

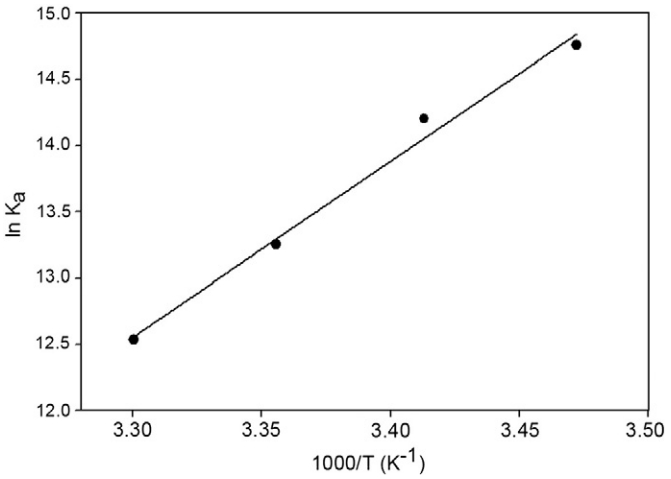

Fig. 4. van't Hoff plot of BLG–NG system.

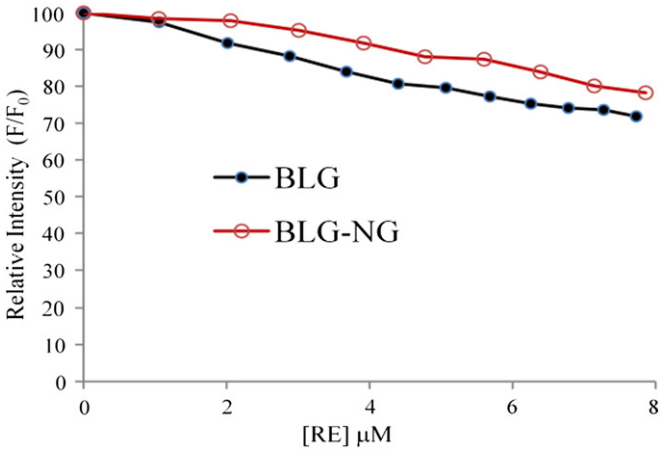

Fig. 5. Relative fluorescence intensities of the BLG in the absence and presence of saturating NG, as a function of RE concentration.

Energy minimization procedure was performed to relieve unfavorable interactions using the steepest descent method [28]. MD simulation studies comprised of equilibration and production phases. In the first stage of equilibration an MD simulation of 100 ps was performed in the NVT ensemble to equilibrate the system. The temperature was maintained at 300 K with the Nose–Hoover thermostat [29,30]. In a second stage of equilibration, a 100 ps NPT equilibration was performed using the Parrinello–Rahman barostat [31] to keep pressure constant in 1.0 bar. The long range electrostatics was treated with the Particle Mesh Ewald (PME) method [32,33] using 1.0 nm cut off. For van der Waals interactions, Lennard-Jones potential with 1.0 nm cut off was employed.

3. Results and discussion

3.1. Fluorescence quenching of BLG

NG is non-fluorescent in phosphate buffer [13]. Fig. 1 displays the emission spectra of BLG in the presence of various concentrations of NG. The fluorescence intensity decreases with the increase in NG concentration, however the rate of quenching decreased with the increase in NG concentration. To distinguish static and dynamic quenching, two methods can be used, such as comparison of the values of K_{sv} at different temperatures and determination of the values of k_Q [12]. At higher temperatures due to faster motions, dissociation of weakly bound complexes increases, amounts of static quenching and consequently, the Stern–Volmer constant decrease.

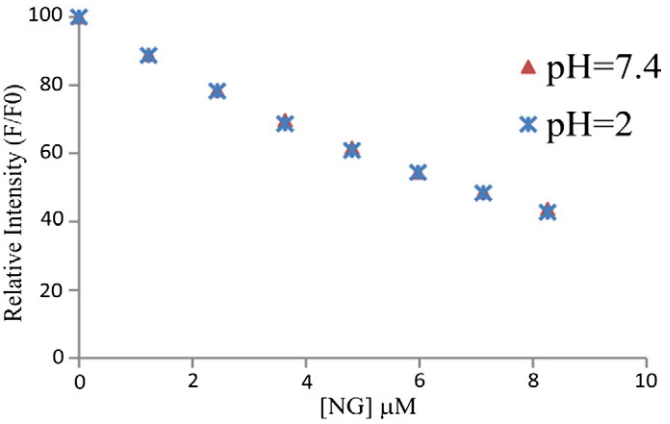

Fig. 6. Influence of acidic pH on the binding of NG to BLG.

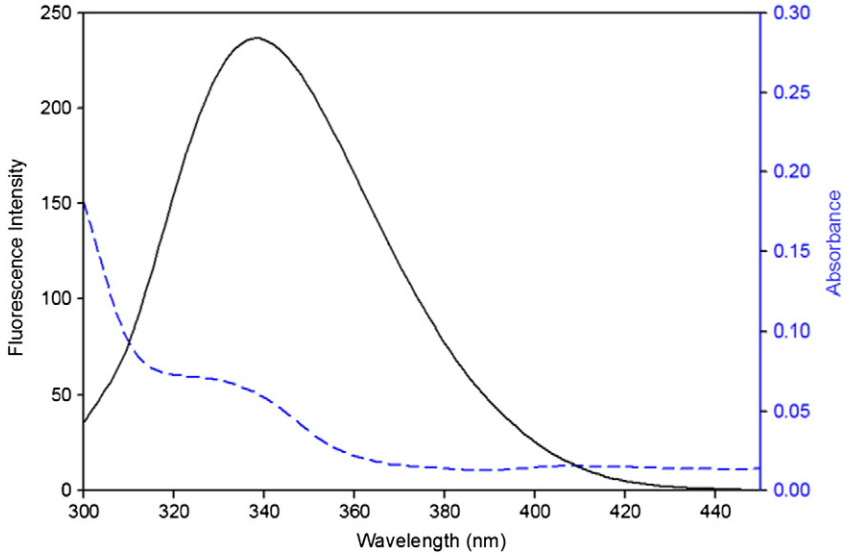

Fig. 7. Overlap emission spectrum (black) and the absorption spectrum (dashed-blue) of BLG with NG as ligand, measured in PBS buffer pH 7.4, $\lambda_{ex} = 280$ nm and [BLG] = [NG] = 10 μM.

The Stern–Volmer plots for the quenching of BLG fluorescence by NG at different temperatures are depicted in Fig. 2 and the estimated K_{sv} and k_Q at different temperatures according to the Eq. (1) are listed in Table 1. Clearly, the values of K_{sv} decreased with the increase of temperature, representing the static quenching mechanism. Moreover, the values of k_Q at all temperatures were far larger than the maximum dynamics quenching constant of various quenchers with biopolymers ($k_Q = 29 \times 10^{10}$ L mol^{-1} s^{-1} [34]), indicating the static process as a main mechanism of quenching.

Based on Eq. (2) the plot of ln[Q] vs. ln$((F_0 - F)/F)$ is represented in Fig. 3. The estimated values of n and K_a at various temperatures are listed in Table 2. The results proved the formation of 1:1 complex and the relatively high binding affinity of NG to BLG.

In order to obtain further information about the energetics of binding process, the thermodynamics binding parameters such as the standard Gibbs free energy, ΔG^0, the standard molar enthalpy, ΔH^0, and the standard molar entropy, ΔS^0, were calculated from the running of binding experiments at various temperatures. According to the relationship, $\Delta G^0 = -RT \ln K_a$, ΔG^0 can be calculated from equilibrium constant, K_a. As the standard enthalpy change doesn't vary significantly over the considered temperature range, the standard enthalpy and entropy change of binding can be estimated from Eq. (6) (van't Hoff equation) and Eq. (7), respectively:

$$\left.{}^{d\ln K_a}\right/_{d(1/T)} = -\Delta H^0/RT \tag{6}$$

$$\Delta S^0 = \left(\Delta G^0 - \Delta H^0\right)/T. \tag{7}$$

Plot of lnK_a vs. $1/T$ (van't Hoff plot) is shown in Fig. 4 and the values of ΔG^0, ΔH^0 and ΔS^0 at different temperatures from 15 to 35 °C are summarized in Table 2.

The thermodynamic parameters of binding reaction could be considered to reveal the driving forces of binding reaction such as hydrophobic, electrostatic, van der Waals interactions and hydrogen bonds.

Table 3
Parameters of Förster non-radiation energy transfer.

	J (M^{-1} · cm^{-1}.nm^4)	E (%)	R_0 (nm)	r (nm)
BLG (variant B)	5.740×10^{13}	44.53	2.070	2.367

The negative value of free energy, ΔG^0, supports that the binding process is spontaneous at all studied temperatures. Also, the negative values of ΔH^0 and ΔS^0 provide that the reaction is enthalpy driven. According to the work of Ross and Subramanian [35] negative value of enthalpy indicates that the main force involved in the binding process is hydrogen bonding and the negative value of entropy points to the importance of van der Waals interactions in solution. Therefore, both hydrogen bonding and van der Waals interactions play an essential role in the binding process of NG to BLG. These interactions can be carried on via the phenolic OH groups and aromatic rings of NG with suitable groups in the binding site of BLG.

3.2. Competitive binding of NG and RE

Three potential binding sites have been identified for ligand binding to BLG: the internal cavity of the β-barrel (calyx), the surface hydrophobic pocket in a groove between the α-helix and the β-barrel, and the outer surface near Trp19–Arg124 [36]. It has been shown that hydrophobic molecules such as fatty acids, vitamins, particularly vitamin D, retinol and palmitate bind to the central cavity of BLG (calyx), [37,38] while, polar aromatic compounds, such as p-nitrophenyl phosphate, 5-fluorocytosine, ellipticine, and protoporphyrin, bind to the outer surface site [39]. A competitive experiment with retinol (RE) was performed to determine if NG also binds to the outer surface of the protein or not. For this purpose, quenching of the BLG in the absence and presence of saturating NG, as a function of RE concentration were measured and the relative quenching of BLG for both systems as a function of RE concentration is shown in Fig. 5.

As shown in this figure the rate of fluorescence quenching of the BLG during the addition of RE, in both systems do not show a significant difference which implies that the binding of NG doesn't affect RE binding and the added RE can totally bind to the BLG. Moreover, the titration pattern of RE binding in the presence of NG in the BLG–NG complex was similar to that of the uncomplexed BLG, which reflected no competition between NG and RE for the same binding site and suggested that RE could bind to the interior cavity of BLG in the presence of NG. Regarding the previous studies and competitive experiment, all together, it could be concluded that NG binds to the outer surface of the protein.

In order to have more evaluation of the NG binding site, the influence of acidic pH on the binding of NG was studied. Previous studies have shown that RE starts to release after 3 h at pH 2 [17]. The release occurs because the EF loop that acts as a gate in the central cavity is in

Table 4
Conformation distribution and amino acid residues involved in BLG–NG interaction for four best docking poses at 300 K. The lowest free binding energy and the related binding constant and number of hydrogen bonds at each cluster are shown in the three last columns.

Pose	No. of members in selected cluster	Involved residues	ΔG°(kJ/mol)	K_a (M^{-1})	H-bonds
1	22	Val(3), Thr(4), Gln(5), Cys(106), Phe(136), Lys(135), Lys(138), Ala(139), Lys(141), Ala(142), Leu(143)	−28.03	7.30×10^4	3
2	7	Thr(18), Trp(19), Tyr(20), Ser(21), Val(43), Glu(44), Leu(156), Glu(158), His(161)	−27.61	6.80×10^4	2
3	100	Pro(38), Leu(39), Val(41), Ile(56), Val(92), Phe(105), Met(107)	−27.42	6.43×10^4	0
4	32	Leu(39), Ala(86), Leu(87), Asn(88), Asn(90), Glu(108), Ser(116)	−27.34	6.35×10^4	4

a closed conformation below pH 6.5 [40]. As shown in Fig. 6, binding measurements on BLG–NG complex at pH 2 revealed that the binding of NG to BLG was unaffected by changes in pH conditions and contrary to RE, the release of NG was not observed at that pH which suggested that NG does not bind to the central calyx.

There are several reports in the literature that obtained similar results corresponding to the binding site of flavonoids on the BLG. By using the effect of pH on the binding of flavonoids to the BLG, and also molecular docking computation, Vuorela et al. showed that flavonoids such as myricetin and daidzein do not bind to the central calyx and they bind to an external part rather than to the central cavity [17]. Liang et al. studied the binding of the natural polyphenolic compound, resveratrol, to bovine BLG and obtained the similar result via the analysis of spectrofluoremetric experimental data [9]. These literature evidences plus the obtained experimental confirmation in this study strongly support the binding of NG to the outer surface of BLG.

3.3. Energy transfer

Fluorescence quenching of BLG by NG indicated the possibility of energy transfer between the protein and the bound NG. In the present study, a solution containing equimolar concentration of BLG and NG (10 μM) was prepared and its UV–vis absorption and fluorescence spectra were recorded. There is a good overlap between the emission spectrum of BLG and the absorption spectrum of NG as shown in Fig. 7. The efficiency of energy transfer and overlapping integration can be calculated using Eqs. (3) and (5). R_0 can be obtained from Eq. (4) using $\kappa^2 = 2/3$, $N = 1.3598$, and $Q_D = 0.08$ [41]. By using the obtained value for E from Eq. (3) and R_0 from Eq. (4), the r value can be calculated. All of the determined parameters are listed in Table 3.

It can be seen from this table that the distance from the bound ligand to the tryptophan residues is less than 7 nm indicating a non-radiative energy transfer mechanism for quenching [20]. Moreover, the value of r is higher than the respective critical distance (R_0), so, the static quenching is more likely responsible for fluorescence quenching than dynamic mechanism that is in agreement with our conclusion corresponding to the decreasing of K_{sv} and k_Q with temperature. The short distance value between bound ligand and the tryptophan residue represents the significant interaction between NG and BLG.

3.4. Molecular docking study

In order to predict the NG binding site, a blind molecular docking computation has been done. Based on positional root mean square deviation of corresponding atoms, the docked conformations were ranked in order of increasing energy, which is called clustering. Cluster analysis predicted 17 different clusters for binding modes of NG to the BLG and the results identified that the first four clusters, ranked with the lowest energy scores, formed 80.5% of total docking runs (161 of 200). Conformation distribution, closed residues involved in the binding to NG, free binding energy, binding constant, and number of hydrogen bonds for lowest docked energy belonging to the first four clusters are listed in Table 4.

According to the docking results, the first pose corresponds to the outer surface site near the α-helix, and the third one represents the hydrophobic pocket (calyx) site. It has been represented that there is no H-bond between NG and BLG in the hydrophobic calyx pose (pose 3). As discussed on the basis of thermodynamic binding parameters, not only van der Waals interactions contributed to the binding process, but also hydrogen bonding played an important role as driving force in the BLG–NG complex formation, verifying the idea that NG cannot bind to the calyx. Additionally, this conclusion that the main binding site of NG on BLG is located in the outer surface pose is also strongly supported by the results of competitive binding experiments and independency of NG binding to pH.

Therefore, binding pose with the lowest docked energy belonging to the top-ranked cluster (pose 1) was selected as the final model for post-docking analysis (MD simulation). The configuration for this interaction

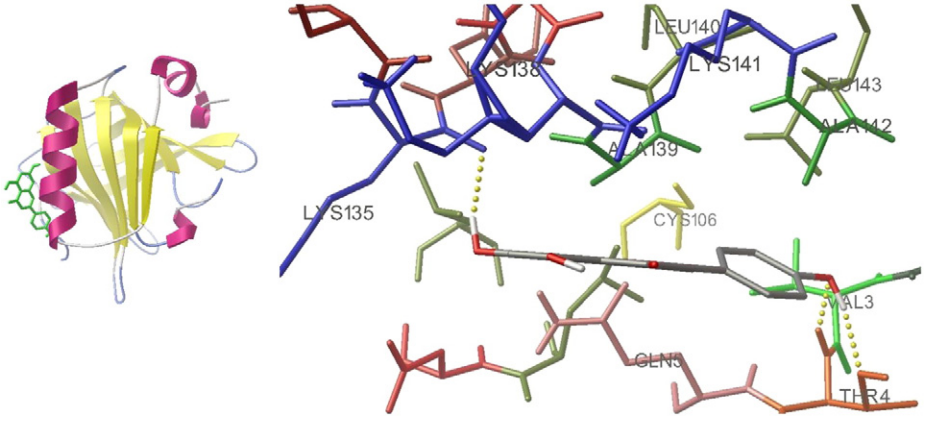

Fig. 8. Best docked conformation and detailed view of the interaction of NG with BLG.

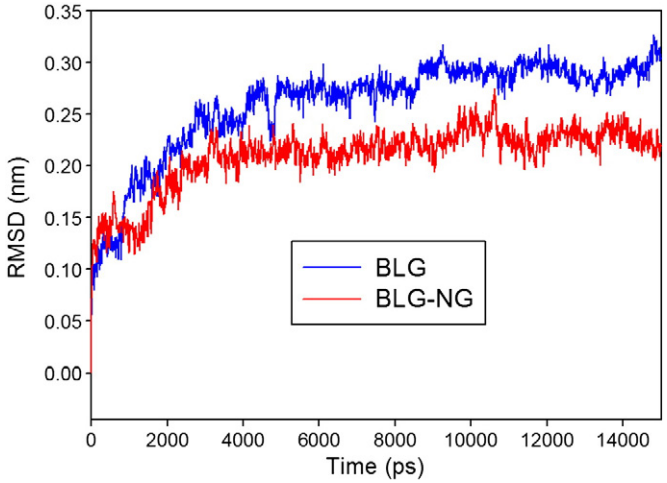

Fig. 9. Time dependence of RMSD (nm) for BLG (blue) and BLG–NG complex (red).

between BLG and NG is exposed in Fig. 8. All closed residues involved in the binding and three hydrogen bonds between the phenolic OH groups of NG and Thr(4), and Lys(135) residues are shown in this figure. The result indicated that NG was adjacent to some hydrophobic residues such as Val, Phe, Ala, Leu, and some polar and electrically charged residues such as Thr, Gln, Cys, and Lys. Therefore, it can be concluded that the interaction of NG with BLG is not only via van der Waals interactions but also through hydrogen bonding formation that is in agreement with the results of thermodynamic analysis.

However, for additional validation on binding site of NG to the BLG, parallel computations on 3NQ9 pdb code of BLG has been done. The resolution of 3NQ9 is 1.9 Å and better than 3NPO (2.2 Å) but it is not ligand free. The results represented the best top-ranked pose in cluster 1 corresponding to the pose near the Glu(158), Val(43), Tyr(20), and Ser(21) in the outer surface rather than near the α-helix or hydrophobic cavity. Nevertheless, the approximate distance between the ligand in this pose and the Trp residue, that are responsible for the energy transfer, was 1.08 nm, which is not in agreement with the distance that can be inferred from the energy transfer experiment (2.34 nm). Moreover, three binding sites have been identified for BLG on basis of experimental evidences [36] that this pose is not one of them. Hence, 3NPO as ligand free case is the best target.

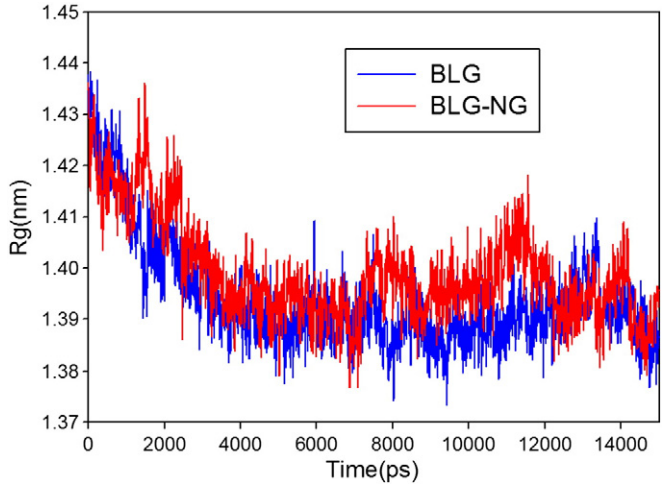

Fig. 10. Time dependence of the radius of gyration (Rg) for the backbone atoms of the free (blue) and bound form (red) of BLG during the simulation.

3.5. Simulation procedures

The lowest energy structure resulting from docking of NG to BLG was selected for the initial structure of 15 ns MD simulation. In order to investigate the stability of the BLG–NG complex and determine the types of interaction involved in the binding reaction, some system properties including root mean square deviations, RMSD, radius of gyration, secondary structure, root mean square fluctuations, RMSF, and hydrogen bonds were investigated. Also, the principal component analysis, PCA, method was applied in order to determine the most important motions contributing to the overall dynamics of the protein during the binding process. In the following, the investigation results of these parameters are presented.

3.5.1. Root mean square deviations

The trajectory stability for both BLG and BLG–NG complex was checked and verified by the analysis of RMSD of backbone atoms of protein from the initial structure, as function of time. It can be seen in Fig. 9 that the RMSD of two systems (BLG and BLG–NG complex) reached equilibrium and oscillated around the average value after about 5000-ps simulation time. In other words, for most of the time (between 5 and 15 ns) the RMSD of protein backbone atoms shows similar trends for both systems indicating their stability and equilibration.

The mean RMSD values of protein backbone atoms from last 4 ns trajectory were 0.293 ± 0.0101 and 0.227 ± 0.0105 nm for BLG and BLG–NG complex, respectively. The lower RMSD value of BLG–NG complex shows that binding of the NG to the BLG decreases the degrees of freedom for protein motions.

3.5.2. Radius of gyration

To have a rough measure for the compactness of a structure, the radius of gyration (R_g) can be calculated. The radius of gyration of the free and bound form of protein was determined and plotted as a function of time, as shown in Fig. 10. In both systems, the R_g values were stabilized at about 5000 ps, indicating that the MD simulation achieved equilibrium after this time. As seen in this figure for both systems, the radius of gyration of backbone atoms decreases. This implies the compacting of BLG structure during the simulation. However, the higher mean value of R_g for the complex represents the reduction of protein compactness due to complexation with NG.

3.5.3. Secondary structure

The secondary structure of BLG after the binding was calculated with the DSSP code [42]. The program generates Fig. 11 that represents the β-sheet, α-helix contents and other secondary structures of BLG during the binding of NG. This represents the insignificant change of secondary structure due to the binding of NG.

3.5.4. Root mean square fluctuations

In order to evaluate local protein mobility the time-averaged root mean square fluctuation (RMSF) values of free BLG and BLG–NG complex were calculated. The results were plotted against residue numbers at the last 4 ns of simulation trajectory. These plots are shown in Fig. 12.

As seen in this figure, the binding of NG restricted the conformational space explored by BLG as assessed by a general reduction of the protein RMSF. In other words, overall reduction in the RMSF values reveals that binding of NG reduces BLG flexibility. The particular regions directly in contact with NG, including Val(3), Thr(4), Gln(5), Cys(106), Phe(136), Ala(139), Lys(141), Ala(142), Leu(143) residues (pointed in Fig. 12) showed more a significant reduction of the RMSF that is related to intermolecular interactions of these residues with the ligand. These residues that are also pointed out in the docking results (Table 4, pose 1) represent insignificant displacement of NG during the simulation.

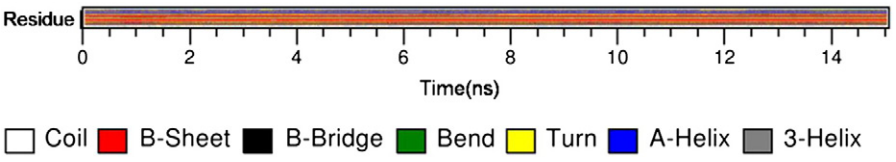

Fig. 11. Variation of the secondary structure of protein versus time for the BLG–NG complex as defined by *do_dssp*.

3.5.5. Hydrogen bond

Hydrogen bond is one of the major forces in ligand binding process. In the Gromacs package, to determine if an H-bond exists, a geometrical criterion is used:

$$r \le r_{HB} = 0.35 \text{ nm}$$
$$\alpha \le \alpha_{HB} = 30^{\circ}.$$

Here, r is the donor–acceptor distance and α is the hydrogen-donor–acceptor angle. The value of $r_{HB} = 0.35$ nm corresponds to the first minimum of the radial distribution function (RDF) of SPC water [43]. Hydrogen bonds between BLG and NG are determined using *g_hbond* program. During the binding process several hydrogen bonds broke and formed. It is found that during the last 4 ns of simulation, the number of hydrogen bonds ranged from 0 to 6 and the average number of hydrogen bonds was 2.755 which is in good agreement with the results of the docking studies. Moreover, the results of simulation revealed that the H bond between the N group of Thr(4) and phenolic OH of NG was maintained in the whole time of simulation whereas the H bond between the OG1 group of Thr(4) and phenolic OH of NG was maintained in 85% of the simulation time. Also, the H bond between the NG and Lys(135) residue disappeared and instead, a new H bond between the ligand and OD1 and OD2 groups of Asp(96) was formed, which was due to the rotation of ligand with respect to the protein.

3.5.6. Principal component analysis (PCA)

PCA transforms the original space of correlated variables into a reduced space of independent variables (i.e. principal components or eigenvectors). In a system of N atoms, there are $3N-6$ modes of possible internal fluctuations (six degrees of freedom are required to describe the external rotation and translation of the system). PCA or essential dynamics simulation helps us to determine what motions contribute most to the overall dynamics of the protein. This method uses the covariance matrix, C, of the atomic coordinates:

$$C_{ij} = \left\langle M_{ii}^{1/2}(x_i - \langle x_i \rangle) M_{jj}^{1/2}\left(x_j - \left\langle x_j \right\rangle\right)\right\rangle$$

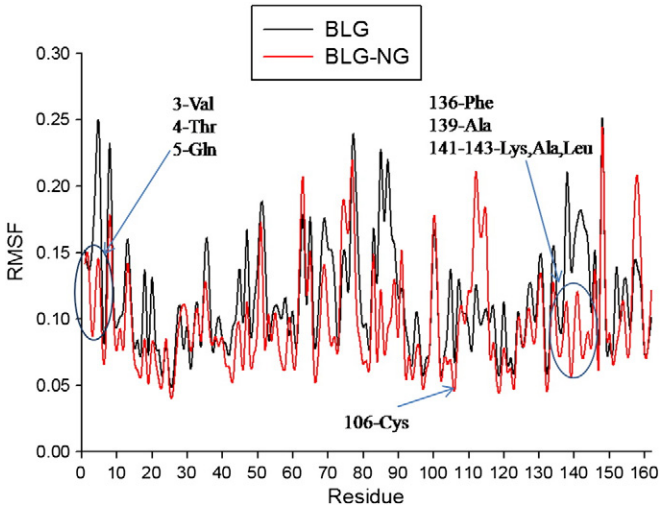

Fig. 12. RMSF of residue of protein from their time-averaged positions for free (black) and bound (red) BLG.

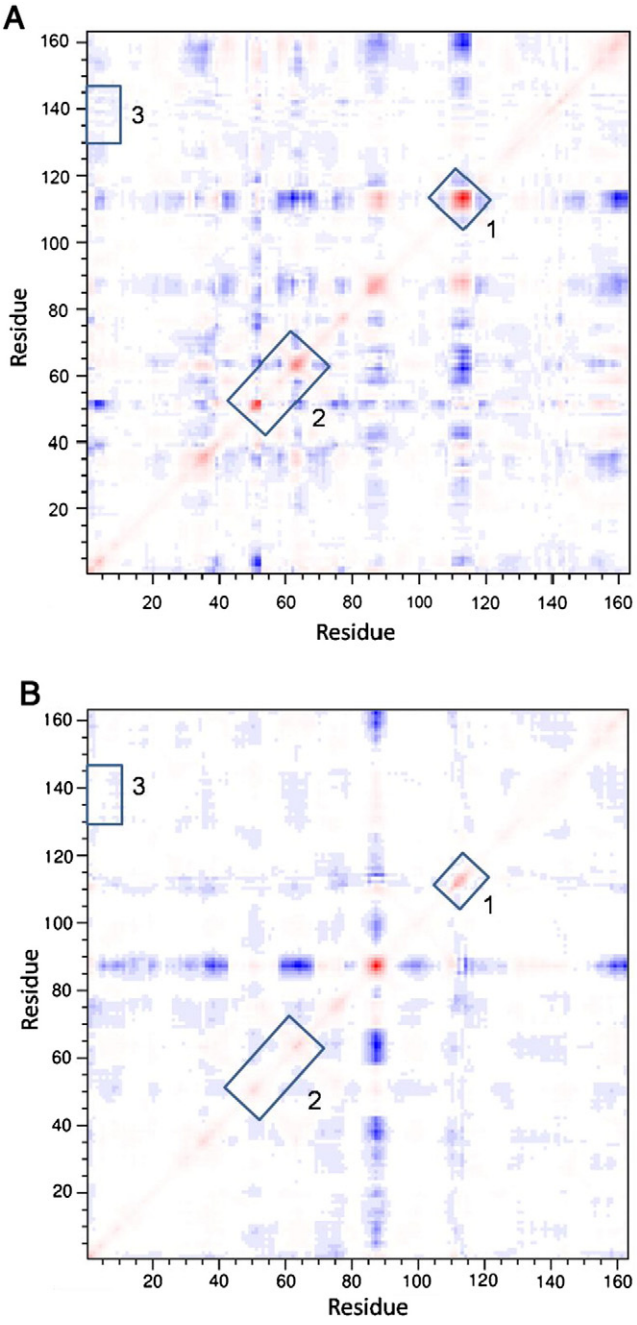

Fig. 13. Correlation maps of (A) free and (B) bound BLG. Correlated (positive) and anticorrelated (negative) motions between atom pairs are represented as color gradients of red and blue, respectively.

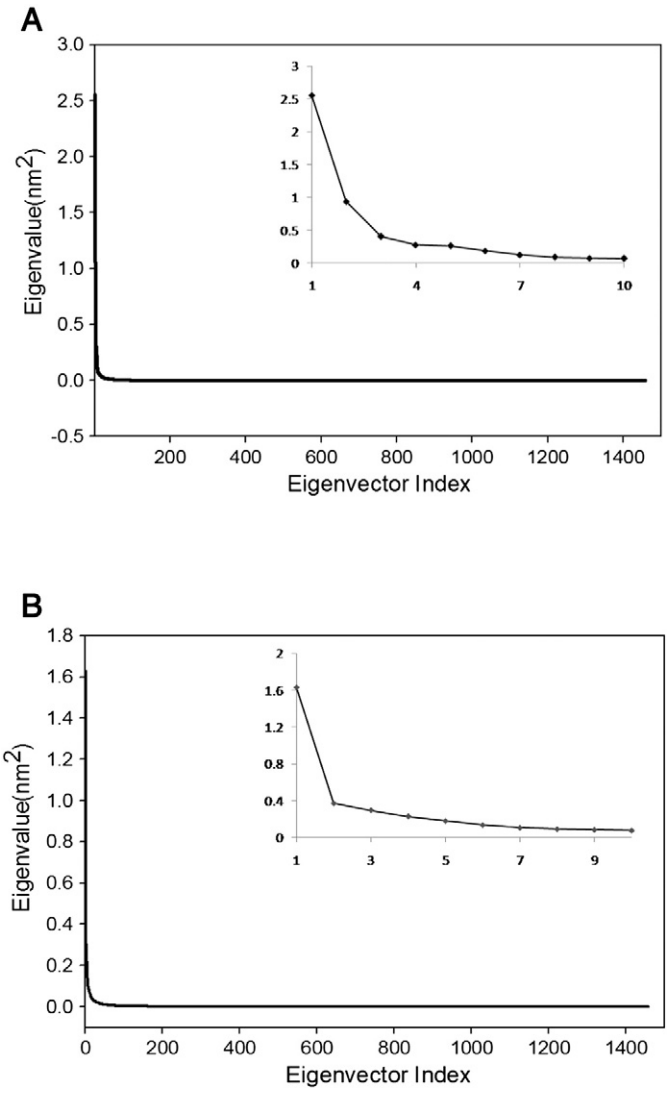

Fig. 14. Eigenvalues of (A) BLG and (B) BLG–NG complex versus the eigenvector indices.

where, M is a diagonal matrix containing the masses of the atoms (mass-weighted analysis) or the unit matrix (non-mass weighted analysis). This matrix describes correlations between all pairs of Cα atoms as they move around their average position and provides a picture of the correlated and anticorrelated motions [43]. Comparison between the correlation maps of free (Fig. 13(A)) and bound BLG (Fig. 13(B)) revealed differences in the motions of the two systems. Investigation of correlation maps showed a reduction in short range correlations (boxes 1 and 2 in Fig. 13) and also, in the binding region anticorrelation motions between residues of (3), (4), (5) and (139), (141), (142), (143) disappeared (box 3 in Fig. 13) due to the binding process. The amplitude and direction of dominant protein motions are identified by the calculation of eigenvectors and eigenvalues of covariance matrix.

Also, the matrix C has been connected to the system constraints. It can be shown that a subspace which is forbidden for the motion is always fully defined by a subset of eigenvector with zero or nearly zero eigenvalues [44]. In this study, the covariance matrix was built for the Cα atoms of protein. Eigenvectors and eigenvalues of free and bound BLG were calculated using *g_covar* program. Eigenvalues of two systems versus the eigenvectors indices are depicted in Fig. 14.

The results showed that only a very small number of eigenvectors (modes of fluctuation) contribute significantly to the overall motion of the protein. Also, the results revealed that for free protein the first 10 eigenvectors account for 76.04% of the global motion whereas for bound BLG the first 10 eigenvectors account for 66.44% of the global motion (inset of Fig. 14). Taken together, correlation maps and correlation matrix analysis reveal the increase of correlated and anticorrelated motions due to binding process. Time evolution of the two first eigenvectors with largest eigenvalues for BLG–NG (PC1 and PC2) is represented in Fig. 15 which indicates that PC1 fluctuated remarkably in comparison to PC2, and therefore this principal movement is responsible for the binding process.

4. Conclusion

In this study, the interaction of NG with BLG was investigated using fluorescence spectroscopy, molecular docking and molecular dynamics simulation. It was shown that the fluorescence of BLG quenched due to the formation of 1:1 complex with NG through static mechanism. Thermodynamic parameters obtained by running the binding experiments at various temperatures indicate the negative sign for both enthalpy and entropy changes and hence, both hydrogen bonding and van der Waals interactions play important roles in the binding process. The results of competitive binding experiments and independency of NG binding to pH revealed that NG does not bind to the central calyx. The molecular docking calculation results revealed that the interaction of NG with BLG is through van der Waals and hydrogen bond interactions. It has been shown that several polar residues such as Val(3), Phe(136), Ala(139), Leu(143), Ala(142) and non-polar residues such as Thr(4), Gln(5), Cys(106), Lys(135), Lys(138), Lys(141) are involved in the binding process. The strong support of docking results by experimental evidences represents the validation of docking calculation.

The result of RMSD and radius of gyration properties obtained by molecular dynamics calculations proved the stability of BLG–NG complex during the simulation and validity of docking results. Analysis of MD data represents the insignificant change of secondary and tertiary structures of BLG due to the binding of NG. The RMSF profiles and hydrogen bond analysis reveal the insignificant movement of ligand from its pose during the MD simulation. The results of PCA proved the increase of both correlated and anticorrelated motions during the binding process. To sum up all these, experimental and molecular modeling results clarified that NG binds to the outer surface of BLG, effectively, which could be a useful guideline for the NG delivery system.

Acknowledgments

The financial supports of the Research Council of University of Isfahan and the Abdus Salam International Center for Theoretical Physics (ICTP, Trieste, Italy) are gratefully acknowledged.

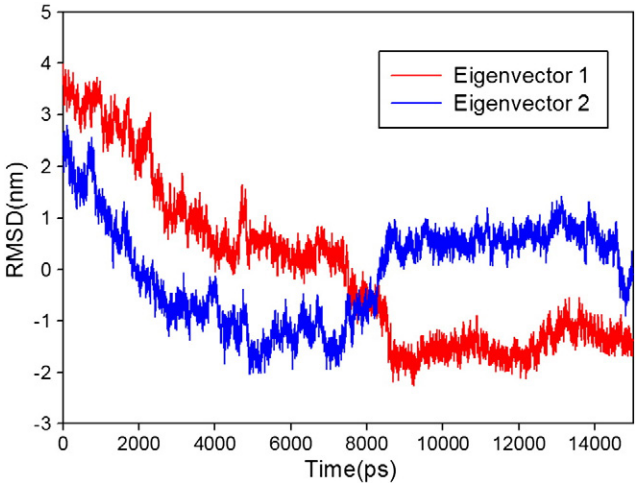

Fig. 15. Time evolution of PC1 and PC2 in BLG–NG complex.

References

[1] N. Cook, S. Samman, Flavonoids—chemistry, metabolism, cardioprotective effects, and dietary sources, J. Nutr. Biochem. 7 (1996) 66–76.
[2] K.E. Heim, A.R. Tagliaferro, D.J. Bobilya, Flavonoid antioxidants: chemistry, metabolism and structure–activity relationships, J. Nutr. Biochem. 13 (2002) 572–584.
[3] E. Middleton, C. Kandaswami, T.C. Theoharides, The effects of plant flavonoids on mammalian cells: implications for inflammation, heart disease, and cancer, Pharmacol. Rev. 52 (2000) 673–751.
[4] M. Nandave, S. Ojha, D. Arya, Protective role of flavonoids in cardiovascular diseases, Nat. Prod. Radiance 4 (2005) 166–176.
[5] R.L. Rouseff, S.F. Martin, C.O. Youtsey, Quantitative survey of narirutin, naringin, hesperidin, and neohesperidin in citrus, J. Agric. Food Chem. 35 (1987) 1027–1030.
[6] T.-R. Li, Z.-Y. Yang, B.-D. Wang, D.-D. Qin, Synthesis, characterization, antioxidant activity and DNA-binding studies of two rare earth(III) complexes with naringenin-2-hydroxy benzoyl hydrazone ligand, Eur. J. Med. Chem. 43 (2008) 1688–1695.
[7] C. Manach, G. Williamson, C. Morand, A. Scalbert, C. Rémésy, Bioavailability and bioefficacy of polyphenols in humans. I. Review of 97 bioavailability studies, Am. J. Clin. Nutr. 81 (2005) 230S–242S.
[8] L. Liang, M. Subirade, β-Lactoglobulin/folic acid complexes: formation, characterization, and biological implication, J. Phys. Chem. B 114 (2010) 6707–6712.
[9] L. Liang, H. Tajmir-Riahi, M. Subirade, Interaction of β-lactoglobulin with resveratrol and its biological implications, Biomacromolecules 9 (2007) 50–56.
[10] A. Mensi, Y. Choiset, H. Rabesona, T. Haertlé, P. Borel, J.-M. Chobert, Interactions of β-lactoglobulin variants A and B with vitamin A. Competitive binding of retinoids and carotenoids, J. Agric. Food Chem. 61 (2013) 4114–4119.
[11] G. Zhang, L. Wang, J. Pan, Probing the binding of the flavonoid diosmetin to human serum albumin by multispectroscopic techniques, J. Agric. Food Chem. 60 (2012) 2721–2729.
[12] S. Bi, L. Yan, B. Pang, Y. Wang, Investigation of three flavonoids binding to bovine serum albumin using molecular fluorescence technique, J. Lumin. 132 (2012) 132–140.
[13] Y.-J. Hu, Y. Wang, Y. Ou-Yang, J. Zhou, Y. Liu, Characterize the interaction between naringenin and bovine serum albumin using spectroscopic approach, J. Lumin. 130 (2010) 1394–1399.
[14] X. Zhang, L. Li, Z. Xu, Z. Liang, J. Su, J. Huang, B. Li, Investigation of the interaction of naringin palmitate with bovine serum albumin: spectroscopic analysis and molecular docking, PLoS One 8 (2013) e59106.
[15] F. Mehranfar, A.-K. Bordbar, H. Parastar, A combined spectroscopic, molecular docking and molecular dynamic study on the interaction of quercetin with β-casein nanoparticles, J. Photochem. Photobiol. B Biol 127 (2013) 100–107.
[16] P. Bourassa, J. Bariyanga, H.A. Tajmir-Riahi, Binding sites of resveratrol, genistein, and curcumin with milk α-and β-caseins, J. Phys. Chem. B 117 (2013) 1287–1295.
[17] L.H. Riihimäki, M.J. Vainio, J.M. Heikura, K.H. Valkonen, V.T. Virtanen, P.M. Vuorela, Binding of phenolic compounds and their derivatives to bovine and reindeer β-lactoglobulin, J. Agric. Food Chem. 56 (2008) 7721–7729.
[18] J. Xiao, F. Mao, F. Yang, Y. Zhao, C. Zhang, K. Yamamoto, Interaction of dietary polyphenols with bovine milk proteins: Molecular structure–affinity relationship and influencing bioactivity aspects, Mol. Nutr. Food Res. 55 (2011) 1637–1645.
[19] E. Dufour, C. Genot, T. Haertlé, β-Lactoglobulin binding properties during its folding changes studied by fluorescence spectroscopy, Biochim. Biophys. Acta Protein Struct. Mol. Enzymol. 1205 (1994) 105–112.
[20] J.R. Lakowicz, Principles of Fluorescence Spectroscopy, Springer, 2009.
[21] J.R. Lakowicz, G. Weber, Quenching of fluorescence by oxygen. Probe for structural fluctuations in macromolecules, Biochemistry 12 (1973) 4161–4170.
[22] J. Min, X. Meng-Xia, Z. Dong, L. Yuan, L. Xiao-Yu, C. Xing, Spectroscopic studies on the interaction of cinnamic acid and its hydroxyl derivatives with human serum albumin, J. Mol. Struct. 692 (2004) 71–80.
[23] M. Frisch, G. Trucks, H. Schlegel, G. Scuseria, M. Robb, J. Cheeseman, J. Montgomery Jr., T. Vreven, K. Kudin, J. Burant, Gaussian 03, Revision B. 03, Gaussian, Inc., Wallingford, CT, 2004.;
M.J. Frisch, et al., Gaussian 03, Revision B. 05, Gaussian, Inc., Pittsburgh, PA, 2003.
[24] G.M. Morris, D.S. Goodsell, R.S. Halliday, R. Huey, W.E. Hart, R.K. Belew, A.J. Olson, Automated docking using a Lamarckian genetic algorithm and an empirical binding free energy function, J. Comput. Chem. 19 (1998) 1639–1662.
[25] D. Van Der Spoel, E. Lindahl, B. Hess, G. Groenhof, A.E. Mark, H.J. Berendsen, GROMACS: fast, flexible, and free, J. Comput. Chem. 26 (2005) 1701–1718.
[26] H. Berendsen, J. Postma, W. Van Gunsteren, J. Hermans, Interaction models for water in relation to protein hydration, Intermol. Forces 11 (1981) 331–342.
[27] A.W. Schuttelkopf, D.M. Van Aalten, PRODRG: a tool for high-throughput crystallography of protein–ligand complexes, Acta Crystallogr. Sect. D: Biol. Crystallogr. 60 (2004) 1355–1363.
[28] B. Hess, C. Kutzner, D. Van Der Spoel, E. Lindahl, GROMACS 4: algorithms for highly efficient, load-balanced, and scalable molecular simulation, J. Chem. Theory Comput. 4 (2008) 435–447.
[29] S. Nosé, A molecular dynamics method for simulations in the canonical ensemble, Mol. Phys. 52 (1984) 255–268.
[30] W.G. Hoover, Canonical dynamics: equilibrium phase-space distributions, Phys. Rev. A 31 (1985) 1695.
[31] M. Parrinello, A. Rahman, Polymorphic transitions in single crystals: a new molecular dynamics method, J. Appl. Phys. 52 (1981) 7182.
[32] T. Darden, D. York, L. Pedersen, Particle mesh Ewald: an N · log (N) method for Ewald sums in large systems, J. Chem. Phys. 98 (1993) 10089.
[33] U. Essmann, L. Perera, M.L. Berkowitz, T. Darden, H. Lee, L.G. Pedersen, A smooth particle mesh Ewald method, J. Chem. Phys. 103 (1995) 8577–8593.
[34] W.R. Ware, Oxygen quenching of fluorescence in solution: an experimental study of the diffusion process, J. Phys. Chem. 66 (1962) 455–458.
[35] P.D. Ross, S. Subramanian, Thermodynamics of protein association reactions: forces contributing to stability, Biochemistry 20 (1981) 3096–3102.
[36] S. Roufik, S.F. Gauthier, X. Leng, S.L. Turgeon, Thermodynamics of binding interactions between bovine β-lactoglobulin A and the antihypertensive peptide β-Lg f142–148, Biomacromolecules 7 (2006) 419–426.
[37] S. Muresan, A. van der Bent, F.A. de Wolf, Interaction of β-lactoglobulin with small hydrophobic ligands as monitored by fluorometry and equilibrium dialysis: nonlinear quenching effects related to protein–protein association, J. Agric. Food Chem. 49 (2001) 2609–2618.
[38] S.-Y. Wu, M.D. Pérez, P. Puyol, L. Sawyer, β-Lactoglobulin binds palmitate within its central cavity, J. Biol. Chem. 274 (1999) 170–174.
[39] E. Dufour, M.C. Marden, T. Haertlé, β-Lactoglobulin binds retinol and protoporphyrin IX at two different binding sites, FEBS Lett. 277 (1990) 223–226.
[40] L. Ragona, F. Fogolari, M. Catalano, R. Ugolini, L. Zetta, H. Molinari, EF loop conformational change triggers ligand binding in β-lactoglobulins, J. Biol. Chem. 278 (2003) 38840–38846.
[41] R.D. Fugate, P.-S. Song, Spectroscopic characterization of β-lactoglobulin–retinol complex, Biochim. Biophys. Acta Protein Struct. 625 (1980) 28–42.
[42] W. Kabsch, C. Sander, Dictionary of protein secondary structure: pattern recognition of hydrogen-bonded and geometrical features, Biopolymers 22 (1983) 2577–2637.
[43] E. Apol, R. Apostolov, H.J.C. Berendsen, A. Van Buuren, P. Bjelkmar, R. Van Drunen, A. Feenstra, G. Groenhof, P. Kasson, P. Larsson, GROMACS user manual version 4.5. 4, Royal Institute of Technology and Uppsala University, Stockholm and Uppsala, Sweden, 2010.
[44] A. Amadei, A. Linssen, H.J. Berendsen, Essential dynamics of proteins, Proteins Struct. Funct. Bioinform. 17 (1993) 412–425.